HIROSAKI UNIVERSITY

Radiation Environment and Medicine 2021 Vol.10, No.2 67–73

REM
Radiat Environ Med

Regular Article

Changes on Distribution of Absorbed Dose Rate in Air Related with Infrastructure Projects on Phu Quoc Island, Vietnam

Kazumasa Inoue[1]*, Masahiro Fukushi[1], Tan Van Le[2], Nguyen Hoang Vu[3], Mizuho Tsukada[1], Mai Ichihara[1], Yoshiaki Taguchi[1] and Hiroaki Sagara[1]

[1]*Tokyo Metropolitan University, 7-2-10 Higashiogu, Arakawa-ku, Tokyo 116-8551, Japan*
[2]*TAM ANH General Hospital at Ho Chi Minh City, 2B Pho Quang Street, Ward 2, Tan Binh District, Ho Chi Minh City 736515, Vietnam*
[3]*University of Medicine and Pharmacy at Ho Chi Minh City, 217 Hong Bang street, district 5, Ho Chi Minh City 70000, Vietnam*

Received 23 November 2020; revised 25 December 2020; accepted 6 January 2021

The absorbed dose rate in air was measured all over Phu Quoc Island, Vietnam after infrastructure projects were undertaken, and changes on dose rates related with these projects were evaluated. The median (range) absorbed dose rate in air for the whole island was 48 nGy/h (19 – 110 nGy/h); as a consequence, dose rate was increased 1.3 times compared to that before infrastructure projects. In the dose rate distribution map, the impacts on dose rate related with constructions of hotels, resorts and roads were clearly displayed. Phu Quoc Island was a sensitive area to changes of absorbed dose rates in air because the original radiation level was low.

Key words: absorbed dose rate in air, car-borne survey, artificial structure, Phu Quoc Island, dose rate distribution map, annual external effective dose

1. Introduction

Environment radiation levels in people's living areas depend primarily on the terrestrial γ-rays emitted from the ground[1)]. Therefore, many researchers have been measuring soil samples which contain natural radionuclides such as ^{40}K, ^{238}U series and ^{232}Th series to determine the environmental radiation levels and radiation risks[2-6)]. Additionally, other researchers have reported that environment radiation levels dramatically changed due to construction projects utilizing buildings materials containing large amounts of natural radionuclides[7-11)].

Phu Quoc Island in Vietnam is located in the southwestern part of Vietnam (Fig. 1). The island has a total area of 593 km^2 and its population was 108,000 in 2019. While the economy was once centered on fishing and agriculture, a fast-growing tourism sector has developed in recent years. This came about from 2014 when the government of Vietnam allowed all foreign tourists to visit the island visa-free for a period of up to 30 days, and the government set Phu Quoc Island as a special administrative region to upgrade it to a provincial city with special administration. Thus, many infrastructure projects have been carried out, including building of several five-star hotels, resorts and roads. The average and median absorbed dose rates in air were previously reported to be 44 nGy/h and 37 nGy/h, respectively[12)]. However, there is a possibility that the absorbed dose rate in air has changed due to these projects.

The estimation of effects on absorbed dose rate in air as related to artificial structures is not easy after the environment is built-up. While some researchers reported environmental radiation levels for Vietnam[9, 13-15)], there are

*Kazumasa Inoue: Tokyo Metropolitan University, 7-2-10 Higashiogu, Arakawa-ku, Tokyo 116-8551, Japan
E-mail: kzminoue@tmu.ac.jp

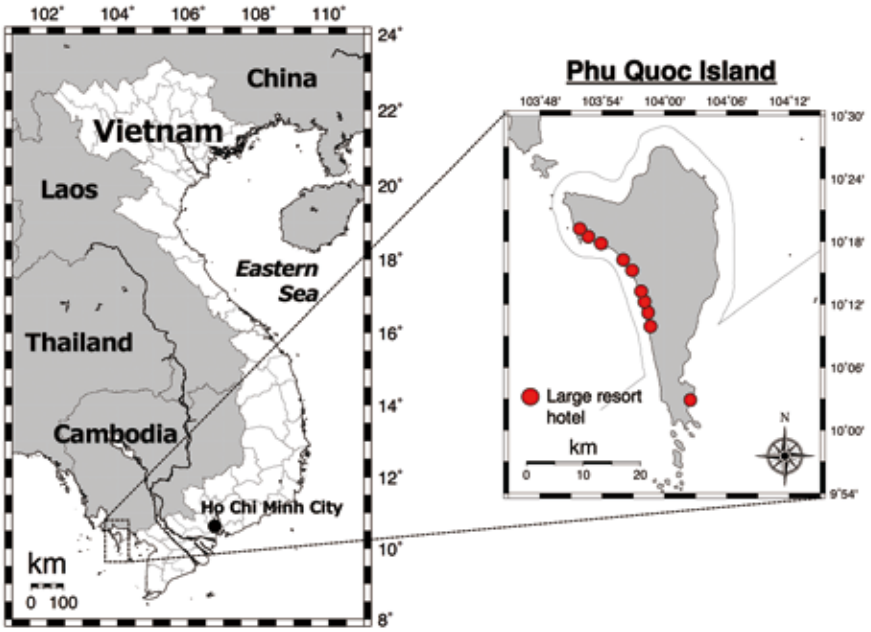

Fig. 1. Maps of Vietnam and Phu Quoc Island, drawn using the Generic Mapping Tools (GMT) of Wessel and Smith[16].

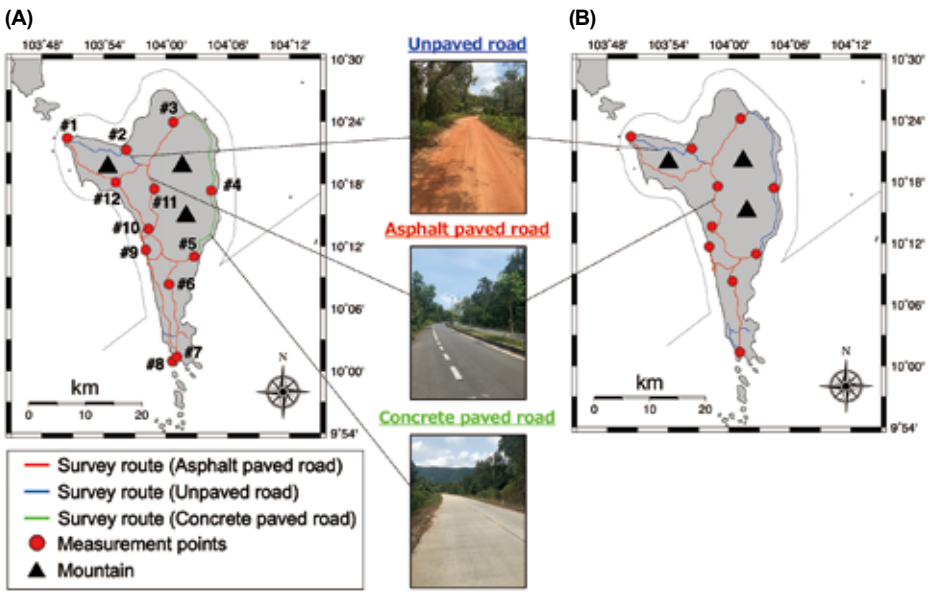

Fig. 2. Maps showing survey routes for measuring the count rates on Phu Quoc Island (A) in 2020 and (B) in 2015[12].

no reports that directly measured changes of radiation level related with changes in urban environments. In this study, a car-borne survey was carried out on Phu Quoc Island in March 2020 (i.e., after the infrastructure projects were completed) and results were compared to previous reported values (i.e., before the projects) to estimate effects on dose rate related with infrastructure projects.

2. Materials and methods

Survey routes

The measurements of the absorbed dose rates in air (nGy/h) were carried out in March 2020 on Phu Quoc Island. The weather was sunny throughout the measurement days, and no rain fell. The survey routes were selected as main roads wherever possible (Fig. 2). This route map was drawn using the Generic Mapping Tools (GMT) created by Wessel and Smith[16].

Car-borne survey

A car-born survey technique is a common method for fast assessment of dose rate in a large area[9, 17, 18]. In the present study, a car-borne survey was carried out using a 3-in×3-in NaI(Tl) scintillation spectrometer with a global positioning system (EMF-211, EMF Japan Co., Osaka, Japan). Measurements of the count rates with gamma-ray energies of 50 keV–3.2 MeV inside the car were performed every 30 s along each route. Simultaneously, latitude and longitude at each measurement point were recorded with the global positioning system. During the survey, precautions were taken that the detector did not move when the car was being driven and the speed of the car was below 25 km h^{-1}. The car windows were kept closed during measurements. The car used for the survey was a Toyota Fortuner with a maximum capacity of five occupants. Four occupants were present in the car during the survey. The photon peak of ^{40}K (E_γ = 1.464 MeV) was used for calibration from the channel number and gamma-ray energy before the measurements. The shielding effect of the car body was estimated by measuring the count rates inside and outside the car at 12 points (red circles in Fig. 2). Measurements were recorded over consecutive 30-s intervals during a total recoding period of 2 min inside and outside the car. Shielding factor was calculated from the correlation between count rates inside and outside the car, and the corrected count rates inside the car were obtained by multiplying the data measured in the car-borne survey with this shielding factor. The gamma-ray pulse height distributions were then measured outside the car for 10 min at 12 points (red circles in Fig. 2). The NaI(Tl) scintillation spectrometer was positioned 1 m above the ground surface for these measurements. The measured gamma-ray pulse height distributions were then unfolded using a 22×22 response matrix method[19] and absorbed dose rates in air were calculated. The calculated dose rates were then used to calculate the dose conversion factor (nGy h^{-1}/cps) from a correlation between dose rates and count rates. The count rates measured by the car-borne survey were multiplied by the obtained dose conversion factor and the absorbed dose rates in air for all of Phu Quoc Island were calculated. All obtained data from the car-borne survey were plotted using GMT[16] as a distribution map of absorbed dose rates in air on Phu Quoc Island. A minimum curvature algorithm was used for the data interpolation by GMT. This is the method for interpolating data by presuming a smooth curved surface from the data of individual points. For a more detailed evaluation, activity concentrations of ^{40}K, ^{238}U and ^{232}Th at all points in Figure 2 (n = 12) were calculated by unfolding the measured gamma-ray pulse height distributions utilizing the 22×22 response matrix method[19]. The energy ranges of 1.39 – 1.54 MeV for ^{40}K, 1.69 – 1.84 MeV and 2.10 – 2.31 MeV for ^{214}Bi (^{238}U-series) and 2.51 – 2.72 MeV for ^{208}Tl (^{232}Th-series) were set and gamma-ray flux densities of 1.464 MeV from ^{40}K, 1.765 MeV and 2.205 MeV from ^{214}Bi and 2.615 MeV from ^{208}Tl were stored, individually[18, 19]. The activity concentrations of ^{40}K, ^{238}U series and ^{232}Th series were then calculated by comparing them with the theoretically evaluated gamma-ray flux density spectrum due to these nuclides[19].

Effects of asphalt pavement and artificial structures on measurements

Some parts of the survey routes were not paved with asphalt (unpaved and concrete paved roads; Figure 2, blue and green lines). Therefore, the measurements of gamma-ray pulse height distributions were carried out for 10 min at 1 m above the asphalt surfaces at points #1, #3, #5 – #8, #10 and #12 (n = 8) in Figure 2 to evaluate the effects of asphalt pavement on the absorbed dose rates in air. A correction factor for asphalt pavement was then calculated from the correlation between count rates on asphalt and unpaved surfaces.

Activity concentrations in soil samples

The soil samples were collected from a layer extending to 15 cm below the ground surface at 12 points (red circles in Fig. 2B). Samples were dried for 24 h at 110 °C and then sieved. Particles less than 2 mm in size were retained for the activity concentration measurement. These particle samples were packed in a U-8 polypropylene container (48 mm diameter×55 mm height) and sealed with araldite glue. The sealed samples were left for 1.5 months to ensure the equilibrium of ^{228}Ra and ^{226}Ra with their decay products in the thorium and uranium series. Activity concentrations of ^{40}K (E_γ = 1.461 MeV), ^{214}Pb (E_γ = 0.351 MeV) and ^{214}Bi (E_γ = 0.609 MeV) for ^{238}U series and ^{228}Ac (E_γ = 911 MeV) for ^{232}Th series in each sample were measured for 30,000 s with a high-purity germanium semiconductor detector (GCD-30185, Baltic Scientific Instruments, Republic of Latvia) placed inside the 100 mm lead shielding to prevent external radiation from affecting the sample analysis. This detector has a relative efficiency of 33% and an energy resolution of 1.73 keV at the gamma-ray energy of 1.33 MeV. The activity concentration of the ^{238}U series was calculated using a weighted average of the activity concentrations of ^{214}Pb and ^{214}Bi.

3. Results and discussion

Correction and dose conversion factors

The correlation between count rates inside and outside the car measured at 12 locations is shown in Figure 3A, and the shielding factor and standard uncertainty[20] were found to be 1.71 and 0.02, respectively. The shielding factor is generally influenced by the type of car, number

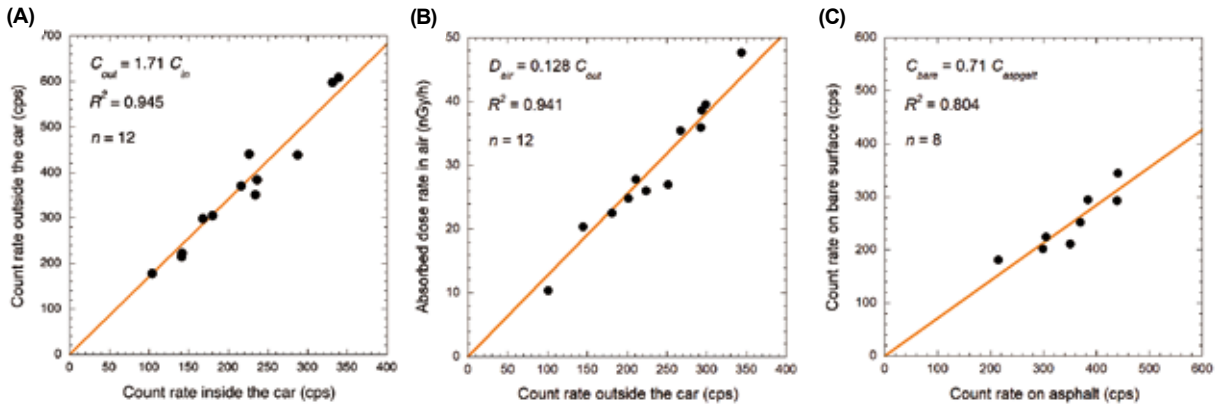

Fig. 3. Correlations between: (A) count rates inside and outside the car; (B) dose rates in air and count rates outside the car; and (C) count rates on bare surface and count rates on asphalt surface.

of passengers and scintillation spectrometer position inside the car. Therefore, the present survey for the 2020 and the 2015 surveys were carried out at the same conditions for all measurements. The calculated shielding factor has been previously reported as ranging from 1.3 – 2.0[9, 17, 21-27], and the presently calculated factor was in this range. Figure 3B shows the correlation between absorbed dose rate in air (nGy/h) calculated using the 22 ×22 response matrix method and count rate outside the car (cps). The dose conversion factor and uncertainty were found to be 0.128 nGy/h/cps and 0.02, respectively. The two correlations shown in Figures 3A and 3B had similar decision coefficients[24, 25]. Here, the absorbed dose rates in air (D_{out}) outside the car 1 m above the ground surface at each measurement point were calculated using Eq. (1):

$$D_{out} = C_{in} \times 1.71 \times 0.128 \quad (1)$$

where C_{in} is count rate inside the car (cps) obtained by the car-borne survey measurements.

Evaluation of the effect of asphalt pavement on measurement

A correction factor for asphalt pavement was calculated from the correlation between count rates measured on the bare surface and the asphalt surface at eight points as shown in Figure 3C, and it was found to be 0.71; as a consequence, the absorbed dose rate in air measured on asphalt was 1.4 times higher than that of the bare surface. The effects of asphalt pavement are strongly dependent on the road structure and the road construction material used. Previously, Inoue *et al.*[9] reported the shielding effect by asphalt pavement at 319 locations in Vietnam, and they found the correction factor for asphalt pavement was 1.37 for southern Vietnam and 0.96 for northern Vietnam. Additionally, these effects depend on the basement geology (i.e., the primary terrestrial gamma radiation dose rate). For example, if the asphalt paved road is constructed on the basement geology with a high dose rate, the artificial structure has been acting as shielding, whereas if the road is constructed on the basement geology with a low dose rate, the artificial structure has been acting as a radiation source[9]. The average and standard deviation of activity concentrations in soil samples (n = 12) were 161 ± 11 Bq/kg for ^{40}K, 11 ± 2 Bq/kg for ^{238}U and 19 ± 12 Bq/kg for ^{232}Th; hence, the obtained average activity concentrations were lower compared to the worldwide averages (400 Bq/kg for ^{40}K, 35 Bq/kg for ^{238}U and 30 Bq/kg for ^{232}Th)[1], and the artificial structures such as roads were acting as a radiation source on Phu Quoc Island.

Distribution of ambient dose rate

The median (range) of absorbed dose rates in air for the whole island (n = 638) was 48 nGy/h (19 – 110 nGy/h) (Fig. 4A). This dose rate was increased 1.3 times compared to the measured value (37 nGy/h; n = 774) in 2015 (i.e., before hotel, resort and road constructions)[12]. The median dose rates (ranges) measured on asphalt paved roads (n = 488), concrete paved roads (n = 74) and unpaved roads (n = 76) were 52 nGy/h (23 – 110 nGy/h), 34 nGy/h (19 – 56 nGy h^{-1}) and 29 nGy/h (20 – 60 nGy/h), respectively. Especially, the dose rate measured on the concrete paved road located on the eastern side of the island (green line in Fig. 2) was increased 1.3 times compared to the value (27 nGy/h) measured on the same route in 2015 when it was unpaved road. Figure 4B shows the cumulative probability distributions of the absorbed dose rate in air for the whole island, and clear differences in the dose rate were seen, and 53% of all measured data in 2020 were increased compared to the 2015 values.

Figures 5A and 5B show the respective dose rate distribution maps drawn using measured data in 2020

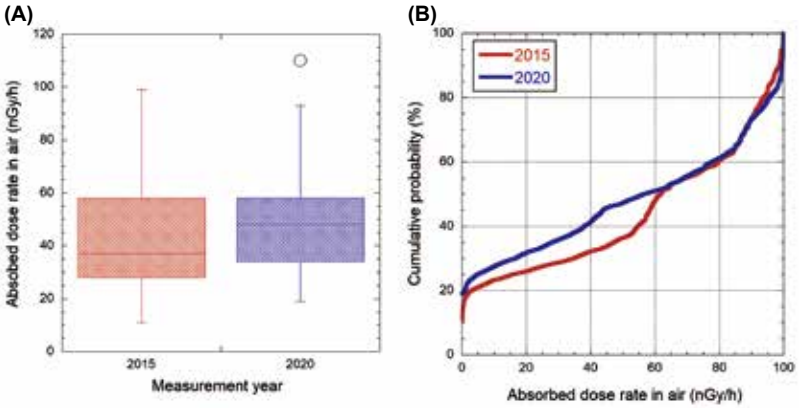

Fig. 4. (A) Calculated absorbed dose rates in air in 2020 and 2015[12] and (B) cumulative probability distributions of absorbed dose rates in air.

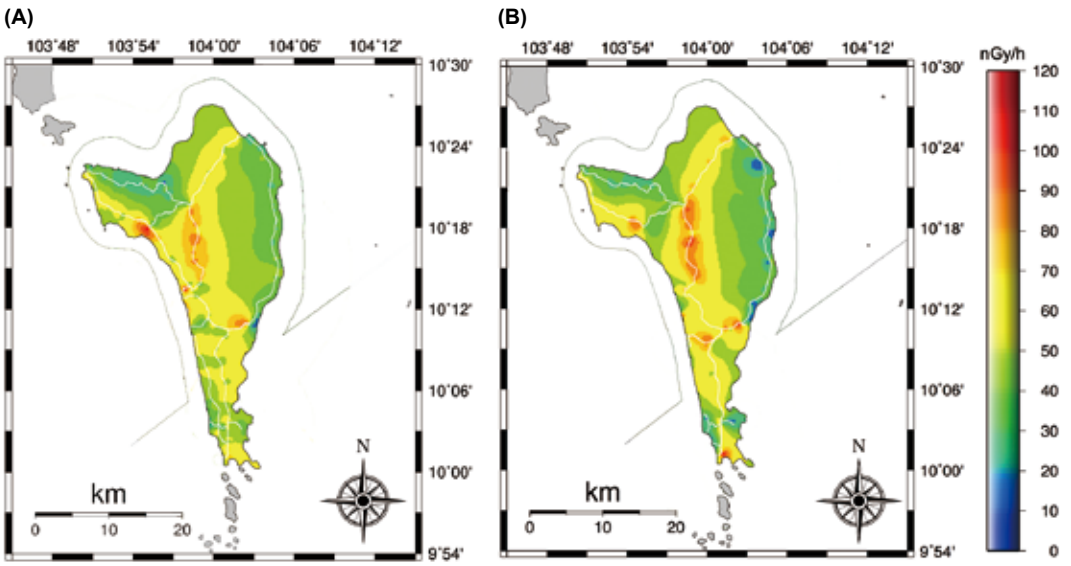

Fig. 5. Distribution maps of absorbed dose rate in air based on the dose rates measured from the car-borne surveys (A) in 2020 and (B) in 2015[12].

(n = 638) and in 2015 (n = 774) on Phu Quoc Island[12]. The maps were drawn with the same magnification and altitude color gradation scale using GMT[16]. A heterogeneous distribution of absorbed dose rates in air was seen. Especially, high absorbed dose rates in air of over 60 nGy/h were observed along the asphalt paved roads which passed from the north to the south. Since these asphalt paved roads had been constructed before 2015, high dose rates had also been observed previously[12]. In the distribution map of 2020 (Fig. 5A), increased dose rates due to road construction were observed on the eastern side of the island reflecting an increased median dose rate as mentioned above.

The maximum relative standard uncertainty of a one-time measurement (30 s) was calculated to be 3.9%. Here, the relative standard uncertainties for the shielding factor, dose conversion factor, traceability of the dose rate and the dose calculation procedure by the response matrix method were given as 2.2%, 2.3%, 4.1% (k = 2) (Pony Industry Co., Ltd., Osaka, Japan), and 5.0% (EMF Japan Co., Osaka, Japan), respectively. Thus, the maximum combined relative standard uncertainty to the estimated absorbed dose rate in air in this study was calculated to be 8.2%.

Figure 6A shows the distribution map of absorbed dose rate in air calculated using a correction factor for asphalt pavement (i.e., 0.71, shown in Fig. 3C) by multiplying D_{out} calculated from Eq. 1. This correction factor was utilized for only data that were measured on asphalt and concrete paved roads. For the detailed evaluation, the dose rate distribution map that used the correction factor for asphalt pavement measured in 2015 is shown in Figure

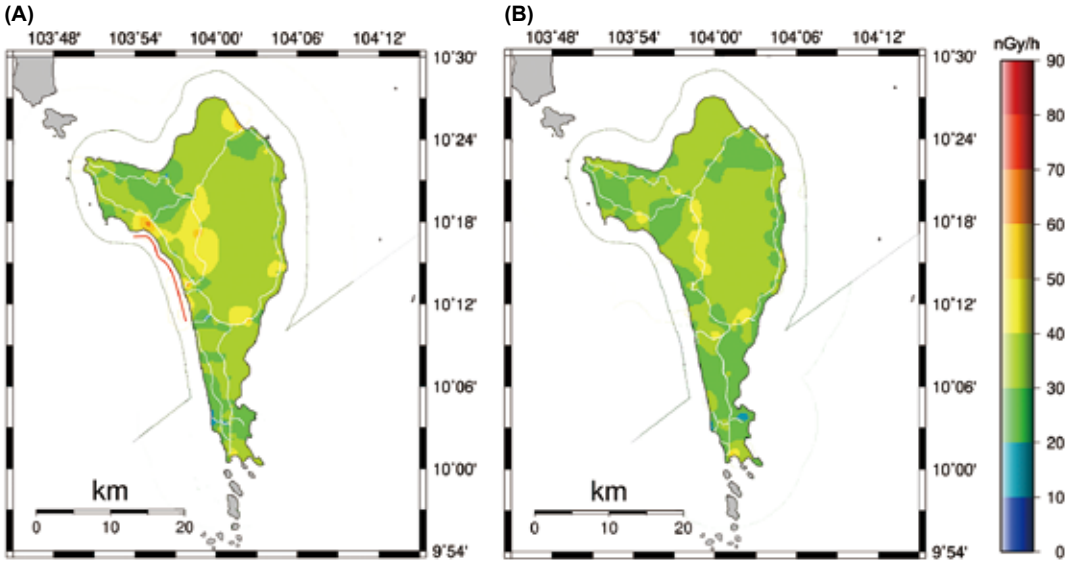

Fig. 6. Distribution maps of absorbed dose rate in air based on the dose rates measured from the car-borne surveys (A) in 2020 and (B) in 2015[12] after using the correction factor for asphalt.

6B. While the previous dose distribution map (Fig. 6B) became a homogeneous dose distribution by excluding the main asphalt paved roads and some villages, the current measured dose distribution map (Fig. 6A) did not display a homogeneous dose distribution. The median of absorbed dose rates after utilizing the correction factor for asphalt pavement were 32 nGy/h for 2020 and 29 nGy/h for 2015. Higher dose rates compared to the previous map were seen along the western coast (red line in Fig. 6A). The line was consistent with the locations of the newly constructed large-scale resort hotels as shown in Figure 1. Thus, the high dose rates measured on the western coast (Fig. 6A) might reflect construction of artificial structures.

External effective dose estimation

The annual external effective dose for Phu Quoc Island was estimated using Eq. 2.

$$E = D_{out} \times DCF \times T \times (Q_{in} \times R + Q_{out}) \times 10^{-6} \quad (2)$$

Here E is the annual external effective dose (mSv/y), D_{out} is the average absorbed dose rate in air (nGy/h), DCF is dose conversion factor from the dose rate to the external effective dose for adults (0.748 ± 0.007 Sv/Gy)[28], T is 8,760 h (24 h × 365 d), and Q_{in} and Q_{out} are indoor (0.8) and outdoor (0.2) occupancy factors, respectively[14]. R is the ratio of indoor dose rate to outdoor dose rate and 1.0 was used for this factor because there is no study that has determined R in Vietnam. The calculated E for the whole Phu Quoc Island was 0.31 mSv/y, and E was slightly increased after resort developments (0.24 mSv/y for 2015)[12]. This value for Phu Quoc Island is 70% of the Vietnam average (0.44 mSv/y, $n = 462$)[9]. Thus, Phu Quoc Island may be a sensitive area for changes in absorbed dose rate in air from newly constructed artificial structures because the original dose rate was low.

4. Conclusion

A car-borne survey was carried out on Phu Quoc Island, Vietnam, in March 2020 after resort and infrastructure developments, and the detailed dose distribution map was made to evaluate changes of dose rate distribution compared to the distribution map made in 2015before such developments. The median absorbed dose rate in air for the whole island in 2020 was 48 nGy/h with the range from 19 to 110 nGy/h, and these values were increased 1.3 times compared to measured values in 2015. Especially, clear changes of absorbed dose rate in air were seen for the eastern side of the island after concrete roads had been built to replace unpaved roads. Additionally, effects from artificial structures related with construction of large-scale resort hotels were observed along the western coast, and 53% of all of measured dose rate data increased compared to values before the developments. In relation with that, annual external effective dose was increased to 0.31 mSv/y. Activity concentrations in soil samples were 161 ± 11 Bq/kg for ^{40}K, 11 ± 2 Bq/kg for ^{238}U and 19 ± 12 Bq/kg for ^{232}Th, which were lower compared to the worldwide averages. Hence, the artificial structures related to the resort and road developments in Phu Quoc

Island had acted as radiation sources.

Funding

This work was funded by the Tokyo Human Resources Foundation of Tokyo Metropolitan Government.

Conflict of Interest

The authors declare that they have no conflict of interest.

References

1. United Nations Scientific Committee on the effects of atomic radiation. UNSCEAR 2000 report to the General Assembly, with scientific annexes. Annex B exposures from natural radiation sources. New York: UNSCEAR; 2000.
2. Al-Hamarneh IF, Awadallah MI. Soil radioactivity levels and radiation hazard assessment in the highlands of northern Jordan. Radiat Meas. 2009;44(1):102–10.
3. Anjos RM, Veiga R, Macario K, Carvalho C, Sanches N, Bastos J, *et al*. Radiometric analysis of Quaternary deposits from the southeastern Brazilian coast. Mar Geol. 2006;229(1):29–43.
4. Arafa W. Specific activity and hazards of granite samples collected from the Eastern Desert of Egypt. J Environ Radioact. 2004;75(3):315–27.
5. Christa EP, Jojo PJ, Vaidyan VK, Anilkumar S, Eappen KP. Radiation dose in the high background radiation area in Kerala, India. Radiat Prot Dosim. 2012;148(4):482–6.
6. Derin MT, Vijayagopal P, Venkatraman B, Chaubey RC, Gopinathan A. Radionuclides and radiation indices of high background radiation area in Chavara-Neendakara placer deposits (Kerala, India). PLoS One. 2012;7(11):e50468.
7. Shimo M, Minato S, Sugino M. A Suruey of Environmental Radiation Aichi, Gifu and Mie Prefectures. J Atom Energ Soc Jap. 1999;41(9):954–64.
8. Sugino M, Shimo M. Survey of environmental radiation dose rates and natural radionuclide concentrations in Gunma Prefecture, Japan. Radioisotopes. 2002;51:543–55.
9. Inoue K, Fukushi M, Van Le T, Tsuruoka H, Kasahara S, Nimelan V. Distribution of gamma radiation dose rate related with natural radionuclides in all of Vietnam and radiological risk assessment of the built-up environment. Sci Rep. 2020;10:12428.
10. Krieger R. Radioactivity of Construction Materials. Betonwerk Fertigteil Tech. 1981;47(8):468–73.
11. Bavarnegin E, Moghaddam MV, Fathabadi N. Natural radionuclide and radiological assessment of building materials in high background radiation areas of Ramsar, Iran. J Med Phys. 2013;38(2):93–7.
12. Le TV, Inoue K, Fujisawa M, Arai M, Fukushi M. Impact on Absorbed Dose Rate in Air from Asphalt Pavement Associated with Transport Infrastructure Developments on Phu Quoc Island, Vietnam. Radiat Environ Med. 2017;6(2):88–93.
13. Hien PD, Hiep HT, Quang NH, Luyen TV, Binh NT, Ngo NT, *et al*. Environmental radionuclides in surface soils of Vietnam. Sci World J. 2002;2:1127–31.
14. Huy NQ, Hien PD, Luyen TV, Hoang DV, Hiep HT, Quang NH, *et al*. Natural radioactivity and external dose assessment of surface soils in Vietnam. Radiat Prot Dosim. 2012;151(3):522–31.
15. Huy NQ, Luyen TV. Study on external exposure doses from terrestrial radioactivity in Southern Vietnam. Radiat Prot Dosim. 2006;118(3):331–6.
16. Wessel P, Smith W. Free software helps map and display data. EOS, Trans Am Geophys Union. 1991;72:441–8.
17. Hosoda M, Tokonami S, Sorimachi A, Monzen S, Osanai M, Yamada M, *et al*. The time variation of dose rate artificially increased by the Fukushima nuclear crisis. Sci Rep. 2011;1:87.
18. Omori Y, Sorimachi A, Gun-Aajav M, Enkhgerel N, Munkherdene G, Oyunbolor G, *et al*. Gamma dose rate distribution in the Unegt subbasin, a uranium deposit area in Dornogobi Province, southeastern Mongolia. Environ Sci Pollut Res. 2019;26:33494–506.
19. Minato S. Diagonal Elements Fitting Technique to Improve Response Matrixes for Environmental Gamma Ray Spectrum Unfolding. Radioisotopes. 2001;50:463–71.
20. Joint Committee for Guides in Metrology. Evaluation of measurement data-guide to the expression of uncertainty in measurement, JCGM 100. 2008:1–116.
21. Inoue K, Tsuruoka H, Le Van T, Fukushi M. Contribution ratios of natural radionuclides to ambient dose rate in air after the Fukushima Daiichi Nuclear Power Plant accident. J Radioanal Nucl Chem. 2015;307:507–12.
22. Inoue K, Hosoda M, Shiroma Y, Furukawa M, Fukushi M, Iwaoka K, *et al*. Changes of ambient gamma-ray dose rate in Katsushika Ward, metropolitan Tokyo before and after the Fukushima Daiichi Nuclear Power Plant accident. J Radioanal Nucl Chem. 2015;303:2159–63.
23. Maedera F, Inoue K, Sugino M, Sano R, Furue M, Shimizu H, *et al*. Natural Variation of Ambient Dose Rate in the Air of Izu-Oshima Island after the Fukushima Daiichi Nuclear Power Plant Accident. Radiat Prot Dosim. 2015;168:561–5.
24. Hosoda M, Inoue K, Oka M, Omori Y, Iwaoka K, Tokonami S. Environmental Radiation Monitoring and External Dose Estimation in Aomori Prefecture after the Fukushima Daiichi Nuclear Power Plant Accident. Jpn J Health Phys. 2016;51:41–50.
25. Hosoda M, Tokonami S, Omori Y, Sahoo SK, Akiba S, Sorimachi A, *et al*. Estimation of External Dose by Car-Borne Survey in Kerala, India. PLoS One. 2015;10:e0124433.
26. Inoue K, Tsuruoka H, Van Le T, Arai M, Saito K, Fukushi M. Impact on ambient dose rate in metropolitan Tokyo from the Fukushima Daiichi Nuclear Power Plant accident. J Environ Radioact. 2016;158-159:1–8.
27. Inoue K, Hosoda M, Fukushi M, Furukawa M, Tokonami S. Absorbed dose rate in air in metropolitan Tokyo before the Fukushima Daiichi Nuclear Power Plant accident. Radiat Prot Dosim. 2015;167:231–4.
28. Moriuchi S, Tsutsumi M, Saito K. Examination on conversion factors to estimate effective dose equivarent from absorbed dose in air for natural gamma radiations. Jpn J Health Phys. 1990;25:121–8.